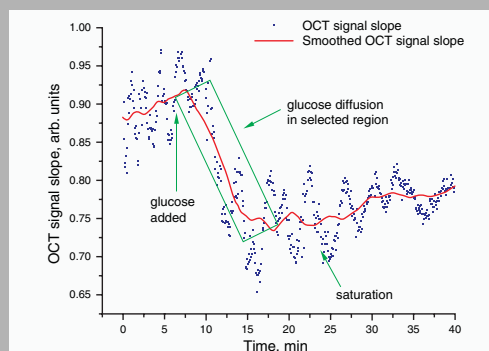


Abstract: Several investigations suggest that the early stages of atherosclerosis are modulated by the selective permeability of the vascular tissue to pro-inflammatory molecules of different molecular weights. Up to date, a few experiments have been performed to study the permeability of arterial tissue to different molecules. This is primarily due to an absence of an experimental technique capable of depth-resolved, accurate and sensitive assessment of arterial permeability. In this paper, we report our pilot results on nondestructive quantification of glucose diffusion in animal arteries *in vitro* by using optical coherence tomography (OCT) technique. Permeability of glucose in animal's aorta was estimated to be $1.43 \pm 0.24 \times 10^{-5}$ cm/sec from five independent experiments. Obtained results suggest capability of OCT technique for highly sensitive, accurate, and nondestructive monitoring and quantification of agents' diffusion in vascular tissues.



OCT signal slope as a function of time recorded from pig aorta during glucose diffusion experiment

© 2007 by Astro Ltd.

Published exclusively by WILEY-VCH Verlag GmbH & Co. KGaA

Quantification of glucose diffusion in arterial tissues by using optical coherence tomography

K.V. Larin,^{1,2,*} M.G. Ghosn,¹ S.N. Ivers,¹ A. Tellez,³ and J.F. Granada³

¹ Biomedical Engineering Program, University of Houston, Houston, Texas, USA

² Saratov State University, Saratov, Russia

³ The Methodist DeBakey Heart Center and The Methodist Hospital Research Institute, Houston, Texas, USA

Received: 2 December 2006, Accepted: 6 December 2006

Published online: 21 December 2006

Key words: noninvasive; diffusion; artery; glucose; optical coherence tomography

PACS: 42.30.-d, 47.57.eb, 42.30.Wb, 42.62.Be

1. Introduction

Accumulation of low-density lipoprotein (LDLs) and other lipid-bearing materials, calcium, and other blood substances in the arterial wall leads to arteriosclerotic disease that is the leading cause of death and disability in developed countries. Significant efforts are currently undertaking to understand, prevent, and cure this disease by many scientists and clinicians around the world. Only in the past decade, Medline® search revealed more than 40 thousands publications devoted to different aspects of the arteriosclerotic research. However, despite all efforts, we still do not completely understand what causes this disease and are unable to significantly reduce associated mortality rate.

There is growing number of evidences suggesting that an increased risk of cardiovascular diseases (CVD) development is not simply caused by the degree of arterial exposure to LDLs but also is determined by arterial susceptibility to different low and high molecular weight substances [1–4]. Regional development of atherosclerosis have been shown to correlate topographically with an increased endothelial permeability [1,5,6].

Several studies suggest that increased arterial permeability relates to the endothelial lining adaptation to different localized shear stresses acting on the wall [7–13]. These results imply that permeability might be increased where the endothelium is exposed to a changing shear stress environment and, thus, that the variability of hemodynamics at the artery wall may actually change the re-

* Corresponding author: e-mail: klarin@uh.edu

gional susceptibility to diseases such as atherosclerosis. Computational and theoretical models of shear-dependent transport of molecules across arterial wall further support these evidences [14–18]. However, up to date, little experimental work has been performed to understand the spatial variation in endothelial permeability and local dynamics of changes in permeability (reviewed in [3,4,12,19]). Therefore, this is an important area for experimental exploration.

Optical-based techniques have great intrinsic potential to study arterial permeability for different molecules. In the past few years, confocal fluorescent microscopy has been applied for assessment of arterial epithelial layer permeability to different molecules *in vitro* [6,20,21]. However, this technique is limited to only the first 50 – 100 μm of tissues. On the other hand, application of other non-optical macro techniques, such as MRI and ultrasound, cannot provide depth-resolved assessment of arterial permeability due to low resolution (e.g. resolution of ultrasound imaging is limited to $\sim 80 - 200 \mu\text{m}$ even with high acoustic frequencies).

Optical coherence tomography (OCT) is relatively new optical imaging technique that provides depth-resolved images of tissues with resolution of about 1 – 20 μm at depths of up to several mm. The first principles of low-coherence interferometry (LCI), a modality of OCT technique, has been described in [22–24]. The first tomographic image of the human eye was obtained in 1991 [25]. Since then, OCT is being actively developed by several research groups for many clinical diagnostic applications (reviewed in [26–28]) including *in vivo* structural imaging of developing cardio-vascular system and CVDs [29–33]. The basic principle of the OCT is to detect backscattered photons from a tissue of interest within a coherence length of the source using a two-beam interferometer. OCT imaging is somewhat analogous to ultrasound B-mode imaging except that it uses light, not sound. Briefly, light from a broadband source (a laser with low coherence) is aimed at objects to be imaged using a beam splitter. Light scattered from the tissue is combined with light returned from the reference arm, and a photodiode detects the resulting interferometric signal. Interferometric signals can be formed only when the optical path length in the sample arm matches the reference arm length within coherence length of the source. By gathering interference data at points across the surface, cross-sectional 2D and 3D images can be formed in real time with resolution of about 1 – 20 μm at depths up to several millimeters, depending on the tissue type. By averaging the OCT images (Fig. 1a) into a single 1D distribution of light in depth in logarithmic scale (Fig. 1b), one can measure the optical properties of tissues by analyzing the profile of light attenuation [34–37].

Recently, we demonstrated capability of OCT technique for monitoring of analytes diffusion in ocular epithelial tissues based on time- and depth-resolved analysis of tissues' scattering properties [38,39]. These results suggest that OCT technique could be successfully applied for functional imaging and quantification of diffusion pro-

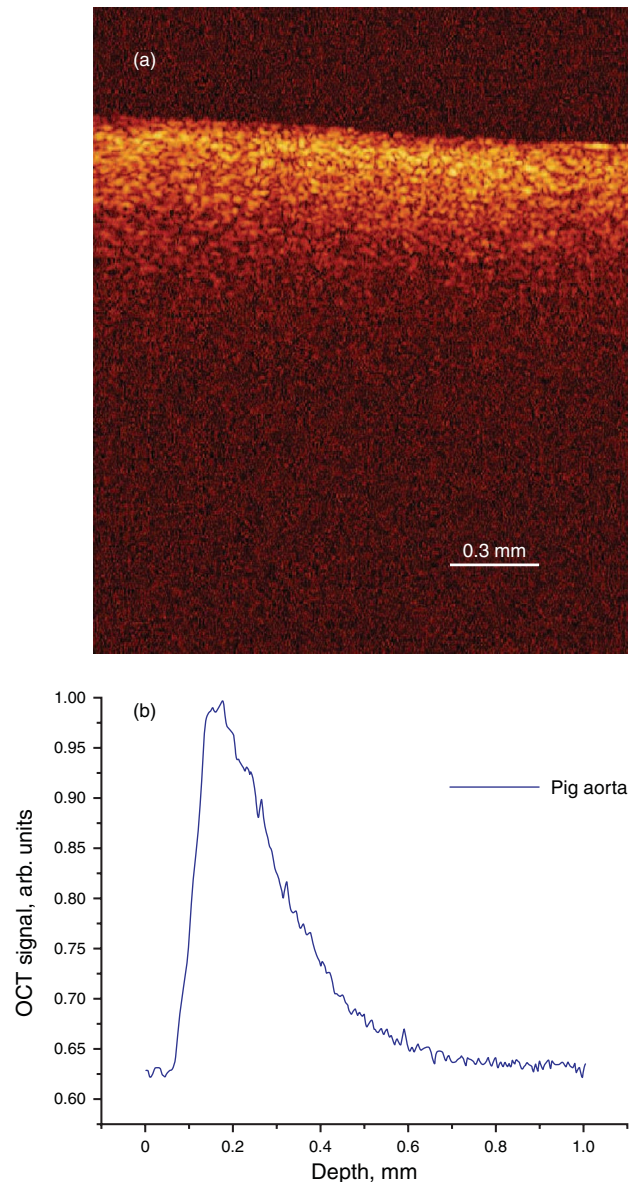


Figure 1 (online color at www.lphys.org) Typical OCT image (a) and corresponding OCT signal (b) recorded from healthy aorta

cesses in tissue-simulating objects and real tissues. In this Letter we report our pilot results on monitoring and quantification of glucose diffusion in healthy aortas of pigs *in vitro*.

2. Materials and methods

2.1. Experimental setup

The experiments were performed using a portable fiber-based OCT system with electro-optical piezo fiber-based

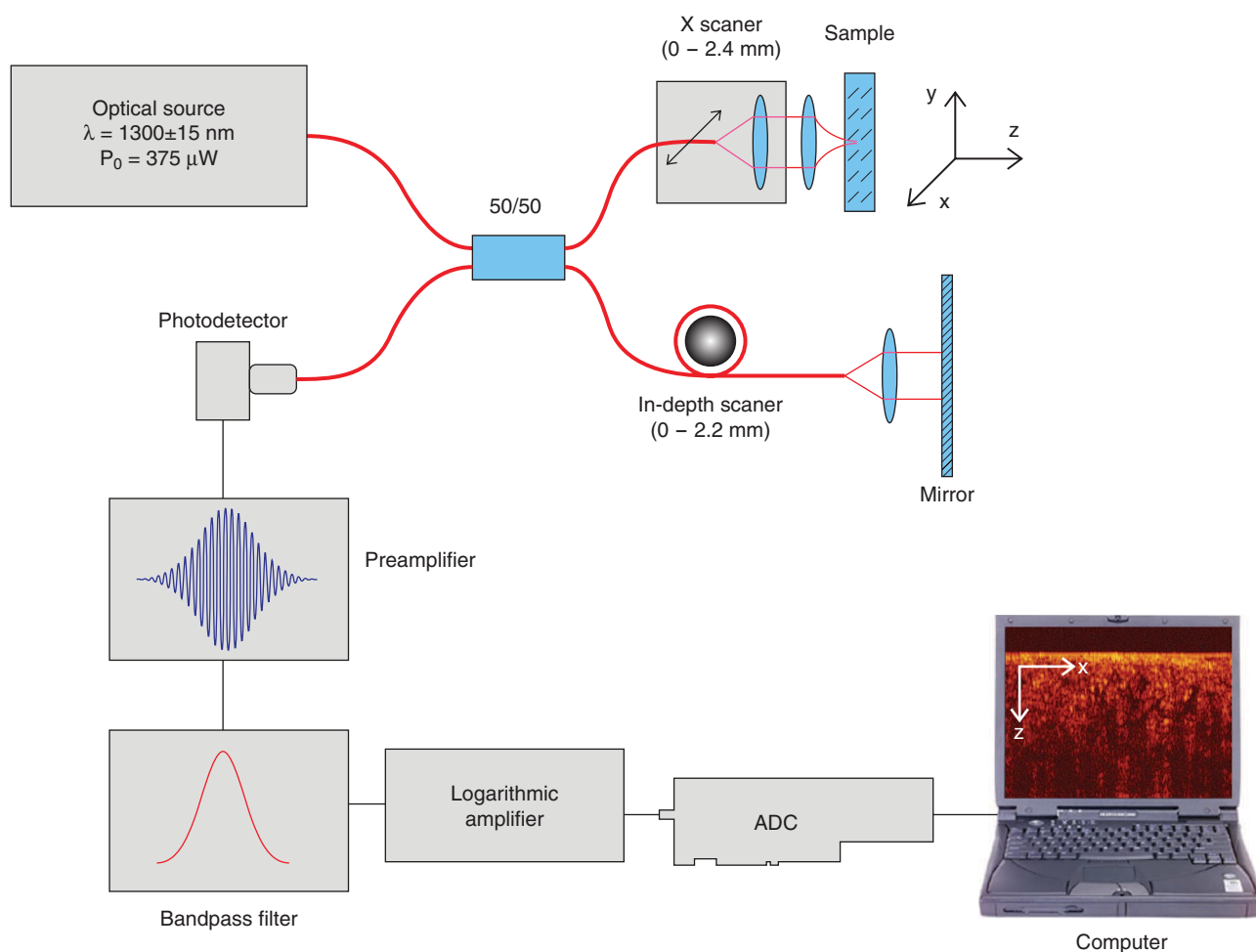


Figure 2 (online color at www.lphys.org) Experimental setup

in-depth scanning system (Fig. 2). The optical source used in this system is a low-coherent broadband, near-infrared (NIR) light source with wavelength of 1300 ± 15 nm and output power of $375 \mu\text{W}$ (Superlum Inc, Russia). Light in the sample arm of the interferometer was directed into the tissues using a single-mode optical fiber that was designed to allow scanning of the sample surface in the lateral direction (X axis). Light scattered from the sample and light reflected from the reference arm mirror formed an interferogram, which was detected by a photodiode. In-depth scanning was produced electronically by piezo-electric modulation of the fiber length. Two-dimensional images were obtained by scanning the incident beam over the sample surface in the lateral direction and in-depth (Z-axial) scanning by the interferometer (Fig. 1a).

The acquired images were 450 by 450 pixels. The in-depth scanning was up to 2.2 mm, while the lateral scanning was 2.4 mm. The full image acquisition rate was approximately 3 sec per image. The operation of the OCT system was fully controlled by PC. The 2D images

were averaged in the lateral direction (over ≈ 1 mm, that was sufficient for speckle-noise suppression) into a single curve to obtain OCT signal in logarithmic scale (Fig. 1b).

2.2. Samples and agents

Experiments were performed using fresh coronary arteries from pigs. The tissues were obtained from our collaborators at The Methodist Research Institute doing terminal animal studies. Once isolated, the tissues were transferred to our lab and experiments were performed within 24 hours. The tissues were kept cooled in a solution of appropriate physiological saline during transportation and storage. Right before experiments, the tissues were placed in a specially designed dish containing a physiological saline of normal room temperature. All experiments were performed at 22°C . Continuous monitoring of tissue optical properties upon topical application of 20%-glucose solution was performed for up to 1 hour in each experiment. Topical application of glucose solution and OCT

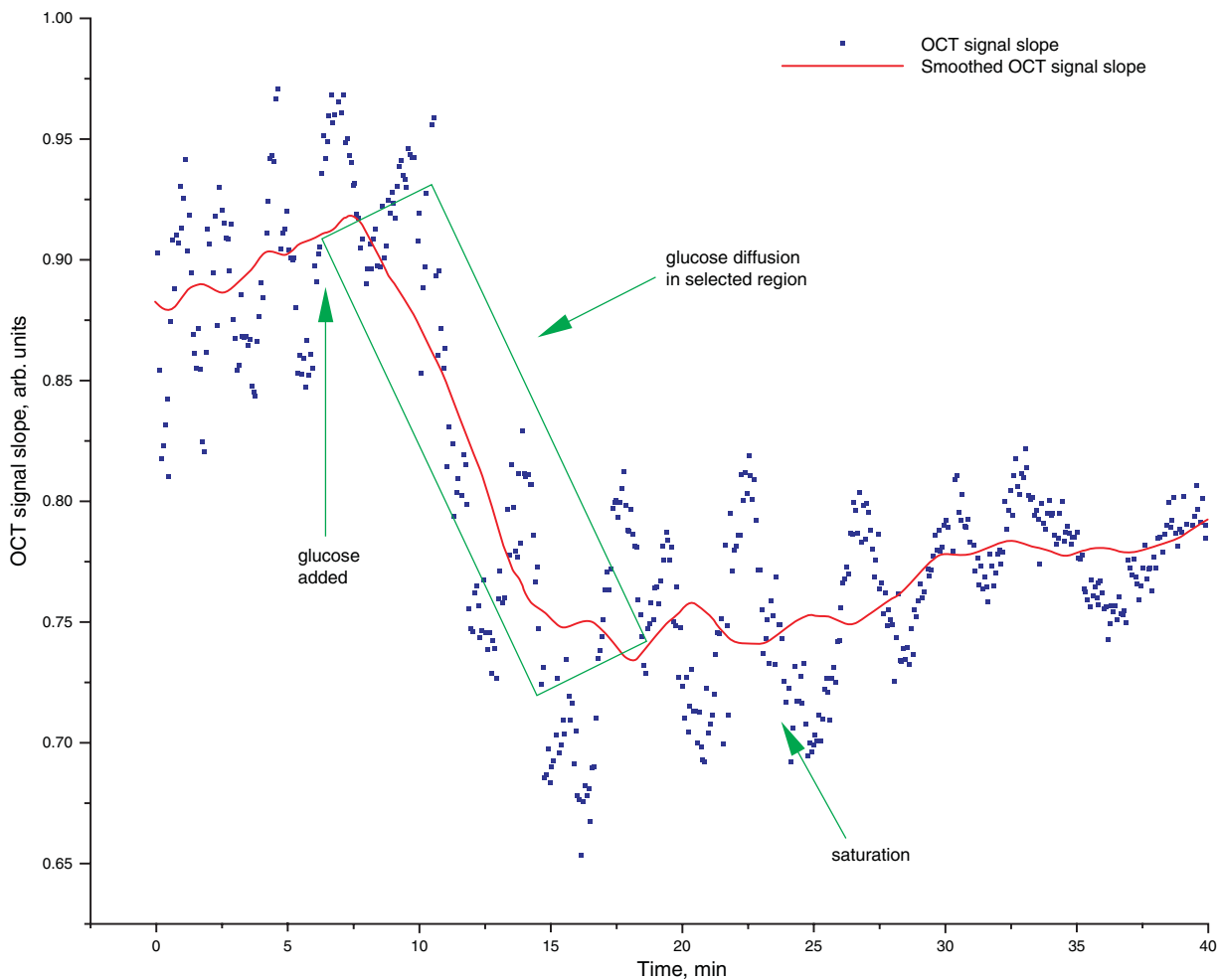


Figure 3 (online color at www.lphys.org) CT signal slope as a function of time recorded from pig aorta during glucose diffusion experiment

functional imaging were performed from endothelial side of the tissues. The epithelial side of the aorta was submerged in a saline solution to minimize dehydration of the tissue. No tissues were used in more than one experiment.

2.3. Methods

Previously, we and other research groups demonstrated that glucose diffusion in epithelial tissues changes its optical properties due to refraction index matching effect and/or changing the local concentrations of scattering particles (and changes in tissue architecture) [34–36,40–43]. Therefore, changes in the in-depth distribution of the tissue scattering coefficient and/or refractive index could be detected by analyzing amplitude and slope of attenuation of OCT signals as a function of depth [34–39,44–46].

The permeability coefficient of the glucose solution in pig's aorta was calculated by analyzing OCT signal

slope at specific tissue's depth as outlined below. The two-dimensional OCT images (Fig. 1a) were averaged in the lateral (X axial) direction into a single curve to obtain an OCT signal that represents one-dimensional distribution of intensity in-depth in logarithmic scale (Fig. 1b). A region in the tissue with minimal distortions of OCT signals was selected and its physical thickness was measured (assuming the refractive index of 1.4). The diffusion of the glucose in this region was monitored in time (commenced as decrease of OCT signal slope [34–36,38,39]) and time of diffusion was recorded. The permeability coefficients were calculated by dividing the measured thickness of the region by the time it took for the glucose solution to diffuse through this region (see Fig. 3).

3. Results and discussion

Typical result obtained during glucose diffusion experiment in pig's aorta is shown in Fig. 3. The OCT signal

Experiment	Permeability coefficient (cm/sec)
Exp.1	1.62×10^{-5}
Exp.2	1.12×10^{-5}
Exp.3	1.66×10^{-5}
Exp.4	1.52×10^{-5}
Exp.5	1.22×10^{-5}
Average \pm SD	$1.43 \pm 0.24 \times 10^{-5}$

Table 1 Permeability coefficients of glucose (20% solution) in experiments with pigs' aorta tissues

slope was calculated from 105 μm region at tissue depth of approximately 52 μm from the surface. A single application of 20% glucose solution ($\sim 1 \text{ mm}^3$) to the endothelial surface of aorta was performed at 6th min after onset of the experiment. Diffusion of glucose solution inside the aorta dynamically changed scattering coefficient and was detected by OCT. The increase in local in-depth glucose concentration resulted in the decrease of the OCT signal slope during the diffusion process. The calculated permeability rate was $1.62 \times 10^{-5} \text{ cm/s}$ in this experiment.

Five pilot experiments were performed with healthy coronary aorta samples from different animals. Glucose permeability rates for these experiments are summarized in Table 1. This table shows, for the first time to the best of our knowledge, permeability coefficient of glucose solution in pig's aorta.

In these pilot experiments we selected to study diffusion of the aqueous solutions of 20%-glucose due several reasons. First, glucose is physiologically important molecule naturally found in blood. Second, the diffusion of glucose in different tissues was extensively studied in our preliminary experiments [34,36,38,39]. Third, glucose is an inert chemical compound and its interaction with tissues has no side effects; thus could be easily applied in future *in vivo* studies. Additionally, according to our preliminary studies, glucose is one of the most potent molecules that significantly affect tissues' scattering properties and, thus, are easy detectable with high signal-to-noise ratio. Nevertheless, we shall investigate diffusion properties of other macromolecules such as albumin and dextran in our future studies. Application of polarization-sensitive methods [47] might additionally improve sensitivity of the system for depth-resolved monitoring and quantification of analytes diffusion (especially low-concentrated macromolecules) in vascular tissues.

Passive diffusion of macromolecules in vascular tissues is critically dependent on the amount and structural organization of smooth muscle cells, collagen and elastic tissue that could vary spatially within a specific tissues segment and from artery to artery according to the disease stage [48]. The regional structural inhomogeneities of arterial walls might result in natural variations of diffusion properties of the same molecule if measured at different geometrical locations in the body. In our experiments,

we tried to preserve the location of excised tissues; nevertheless, the regional ultrastructural differences of arterial walls might result in the observed standard deviation of glucose permeability measured from five different animals.

Recently, several studies suggested that vascular inhomogeneities is reflected not only in variations of geometrical permeability but also in anisotropic transport of macromolecules in the same region [49,50]. The difference of molecular transport in the planar versus the transmural directions is an important topic of investigation and could be successfully accomplished by scanning of the samples in two dimensions. Three-dimensional quantification of molecular diffusion in vascular tissues will allow experimental assessment not only in permeability coefficients (cm/s) reported in this Letter, but also diffusion coefficients (cm^2/s) that might not be a linear extension of the permeability coefficient.

As we mentioned above, the formation of a clot on the surface of a complex atherosclerotic lesion is responsible for the majority of acute coronary events. There are evidences in the literature that complex atherosclerotic lesions undergo a dynamic process of remodeling during the process of plaque progression. These involve significant structural modification of vasculature at the site of atherosclerotic lesions, and, thus, might change glucose permeability coefficients. Therefore, the patterns of glucose diffusion in healthy and diseased tissues might provide a basis for tissues characterization and early diagnosis. Recently, we have developed a vulnerable plaque model in pigs [51]. One of the significant implications of the reported studies will be characterization of plaque vulnerability in the next set of our experiments.

4. Conclusions

In this Letter we demonstrate results of the first nondestructive quantification of arterial permeability to aqueous solution of glucose. The average permeability coefficient of 20% glucose solution was found $1.43 \pm 0.24 \times 10^{-5}$ calculated from five independent experiments. Since development of cardio-vascular diseases is associated with structural and composite alternations of vascular tissues, the proposed method could potentially be applied for tissues characterization and early diagnosis. Our future studies will be focused on monitoring and quantification of molecular permeability in healthy and diseased vascular structures.

References

- [1] M.H. Friedman and D.L. Fry, *Atherosclerosis* **104**, 189 (1993).
- [2] J.M. Tarbell, *Ann. Rev. Biomed. Eng.* **5**, 79 (2003).
- [3] A.I. Goblief, *Cardiovascular Pathol.* **14**, 181 (2005).
- [4] E. Falk, *J. Am. College Cardiol.* **47**, C7 (2006).

- [5] E.M. Pedersen, A.P. Yoganathan, and X.P. Lefebvre, *J. Biomech.* **25**, 935 (1992).
- [6] S.D. Proctor, D.F. Vine, and J.C.L. Mamo, *Arteriosclerosis Thrombosis Vascular Biol.* **24**, 2162 (2004).
- [7] D.D. Duncan, C.B. Barger, S.E. Borchardt, O.J. Deters, S.A. Gearhart, F.F. Mark, and M.H. Friedman, *ASME J. Biomech. Eng.* **112**, 183 (1990).
- [8] H. Jo, R.O. Dull, T.M. Hollis, and J.M. Tarbell, *Am. J. Physiol. Heart Circ. Physiol.* **260**, H1992 (1991).
- [9] E.M. Pedersen, M. Agerbæk, I.B. Kristensen, and A.P. Yoganathan, *Eur. J. Vascular Endovascular Surgery* **13**, 443 (1997).
- [10] O. Ogunrinade, G.T. Kameya, and G.A. Truskey, *Ann. Biomed. Eng.* **30**, 430 (2002).
- [11] H.A. Himburg, D.M. Grzybowski, A.L. Hazel, J.A. LaMack, X.-M. Li, and M.H. Friedman, *Am. J. Physiol. Heart Circ. Physiol.* **286**, H1916 (2004).
- [12] K.S. Cunningham and A.I. Gotlieb, *Lab. Invest.* **85**, 9 (2005).
- [13] C.M. Prado, S.G. Ramos, J.C.F. Alves-Filho, J. Elias, Jr., F.Q. Cunha, and M.A. Rossi, *J. Hypertension* **24**, 503 (2006).
- [14] M. Lei, C. Kleinstreuer, and J.P. Archie, *ASME J. Biomech. Eng.* **119**, 343 (1997).
- [15] M.Z. Darbeau, R.J. Lutz, and W.E. Collins, *Asaio J.* **46**, 669 (2000).
- [16] C.R. Ethier, *Ann. Biomed. Eng.* **30**, 461 (2002).
- [17] A.L. Hazel, D.M. Grzybowski, and M.H. Friedman, *Ann. Biomed. Eng.* **31**, 412 (2003).
- [18] M. Prosi, P. Zunino, K. Perktold, and A. Quarteroni, *J. Biomech.* **38**, 903 (2005).
- [19] A.M. Shaaban and A.J. Duerinckx, *Am. J. Roentgenology* **174**, 1657 (2000).
- [20] N.C. Chesler and O.C. Enyinna, *ASME J. Biomech. Eng.* **125**, 389 (2003).
- [21] P.M.A. van Haaren, E. VanBavel, H. Vink, and J.A.E. Spaan, *Am. J. Physiol. Heart Circ. Physiol.* **289**, H2503 (2005).
- [22] V.P. Linnik, *Trudy AN SSSR* **1**, 208 (1933), in Russian.
- [23] P.A. Flourney, *App. Opt.* **11**, 1907 (1972).
- [24] H.H. Gilgen, R.P. Novak, R.P. Salathe, W. Hodel, and P. Beaud, *J. Lightwave Tech.* **7**, 1225 (1989).
- [25] D. Huang, E.A. Swanson, C.P. Lin, J.S. Schuman, W.G. Stinson, W. Chang, M.R. Hee, T. Flotte, K. Gregory, C.A. Puliafito, and J.G. Fujimoto, *Science* **254**, 1178 (1991).
- [26] A.F. Fercher, W. Drexler, C.K. Hitzenberger, and T. Lasser, *Rep. Prog. Phys.* **66**, 239 (2003).
- [27] J.M. Schmitt, *IEEE J. Sel. Top. Quantum Electron.* **5**, 1205 (1999).
- [28] P.H. Tomlins and R.K. Wang, *J. Phys. D* **38**, 2519 (2005).
- [29] S. A. Boppart et al., *Circulation* **94**, 2828 (1996).
- [30] T.M. Yelbuz, M.A. Choma, L. Thrane, M.L. Kirby, and J.A. Izatt, *Circulation* **106**, 2771 (2002).
- [31] B.D. MacNeill, B.E. Bouma, H. Yabushita, I.K. Jang, and G.J. Tearney, *J. Nucl. Cardiol.* **12**, 460 (2005).
- [32] F.J. van der Meer, D.J. Faber, D.M.B. Sasso, M.C. Aalders, G. Pasterkamp, T.G. van Leeuwen, *IEEE Trans. Med. Imag.* **24**, 1369 (2005).
- [33] G.J. Tearney, I.K. Jang, and B.E. Bouma, *J. Biomed. Opt.* **11** (2006).
- [34] R.O. Esenaliev, K.V. Larin, I.V. Larina, and M. Motamedi, *Opt. Lett.* **26**, 992 (2001).
- [35] K.V. Larin, M.S. Eleddrisi, M. Motamedi, and R.O. Esenaliev, *Diabetes Care* **25**, 2263 (2002).
- [36] K.V. Larin, M. Motamedi, T.V. Ashitkov, and R.O. Esenaliev, *Phys. Med. Biology* **48**, 1371 (2003).
- [37] M. Kinnunen, R. Myllylä, T. Jokela, and S. Vainio, *Appl. Opt.* **45**, 2251 (2006).
- [38] M. Ghosn, V.V. Tuchin, and K.V. Larin, *Opt. Lett.* **31**, 2314 (2006).
- [39] K.V. Larin and M. Ghosn, *Quantum Electron.* **36**, 1083 (2006).
- [40] V.V. Tuchin, I.L. Maksimova, D.A. Zimnyakov, I.L. Kon, A.H. Mavlyutov, and A.A. Mishin, *J. Biomed. Opt.* **2**, 401 (1997).
- [41] A.T. Yeh and J. Hirshburg, *J. Biomed. Opt.* **11**, 14003 (2006).
- [42] V.V. Tuchin, *Optical Clearing of Tissues and Blood* (SPIE Press, 2005), Vol. PM 154.
- [43] V.V. Tuchin, *J. Phys. D* **38**, 2497 (2005).
- [44] K.V. Larin, T. Akkin, R.O. Esenaliev, M. Motamedi, and T.E. Milner, *Appl. Opt.* **43**, 3408 (2004).
- [45] R.K. Wang, X. Xu, V.V. Tuchin, and J.B. Elder, *J. Opt. Soc. Am. B* **18**, 948 (2001).
- [46] V.V. Tuchin, X.Q. Xu, and R.K. Wang, *Appl. Opt.* **41**, 258 (2002).
- [47] V.M. Gelikonov and G.V. Gelikonov, *Laser Phys. Lett.* **3**, 445 (2006).
- [48] C.P. Winlove, K.H. Parker, N.C. Avery, and A.J. Bailey, *Diabetologia* **39**, 1131 (1996).
- [49] C.-W. Hwang and E.R. Edelman, *Circ. Res.* **90**, 826 (2002).
- [50] S. Weinbaum, P. Gatos, R. Pfeffer, G.B. Wen, M. Lee, and S. Chien, *J. Theor. Biol.* **135**, 1 (1988).
- [51] J.F. Granada, P.R. Moreno, A.P. Burke, D.G. Schulz, A.E. Raizner, and G.L. Kaluza, *Coron. Artery Dis.* **16**, 217 (2005).